JOURNAL OF MATERIALS SCIENCE 19 (1984) 2373–2377

Load relaxation of stainless steel Type AISI 304 near 563 K

F. POVOLO
Comisión Nacional de Energía Atómica, Dto. de Materiales, Av. del Liberatador 8250, (1429) Buenos Aires, Argentina

R. TINIVELLA
Universidad Tecnológica Nacional, Facultad Regional S. Nicolás, (2900) S. Nicolás, Argentina

Load relaxation data reported by Anciaux, near 563 K, on mill-annealed Type AISI 304 stainless steel are interpreted in terms of a general expression which describes stress relaxation as thermally activated dislocation motion over precipitates. Several physical parameters are obtained from the stress -strain rate curves and it is shown that for some stress relaxation curves the internal stress does not remain constant during the relaxation.

1. Introduction

Anciaux [1] has published load relaxation data, near 563 K, for three austenitic stainless steels. The tests were conducted in a strain-controlled servo-hydraulic test machine near the yield point strain levels. For stainless steel Type AISI 304 Anciaux reported the stress–strain rate trajectories, at different strain levels, for mill-annealed specimens. The shape of the log stress–log strain rate stress relaxation curve was found to depend on the strain level, but no explanation was given for this behaviour. Furthermore, the curves did not translate on to a master stress–strain rate trajectory.

Povolo and Tinivella [2] have recently interpreted stress relaxation measurements, performed at 773 K in bending, in Type AISI 304 stainless steel in terms of a stress-partitioned power law. For certain thermomechanical treatments it was found that the internal stress depended on the applied stress since the microstructure recovered during the relaxation.

It is the purpose of this paper to interpret Anciaux's data in terms of a general expression that describes the stress relaxation behaviour as a thermally activated process. Several physical parameters will be obtained from the stress relaxation curves and a comparison will be made with the results obtained in bending.

2. Results

The experimental details and the composition of the alloy used have been described by Anciaux [1]. Fig. 1, taken from Fig. 6 of [1], shows the load relaxation curves obtained in mill-annealed AISI 304 near 563 K. The last number on each curve indicates the total applied strain during relaxation.

All specimens were obtained at the same temperature; for specimens T5 the tests were performed at 568 K, for specimens R10 at 566 K, and for specimen R8 at 558 K.

From Fig. 1 it may be seen that the stress–srain rate trajectories are mainly described by concave upward curves, except for specimens T5/2% and T5/0.3% where the concavity changes at low strain rates. Povolo and Tinivella [2] have observed either concave upward or concave downward stress–strain rate trajectories during stress relaxation measurements, in bending, on AISI 304 at 773 K. The concave upward or linear trajectories have been interpreted in terms of the Johnston–Gilman equation [3], and the concave downward ones in terms of Hart's [4] equation for high homologous temperatures. A similar procedure will be used to interpret the curves of Fig. 1 and will be extended to those curves showing a mixed curvature.

The very well known equation that describes

0022–2461/84 $03.00 + .12

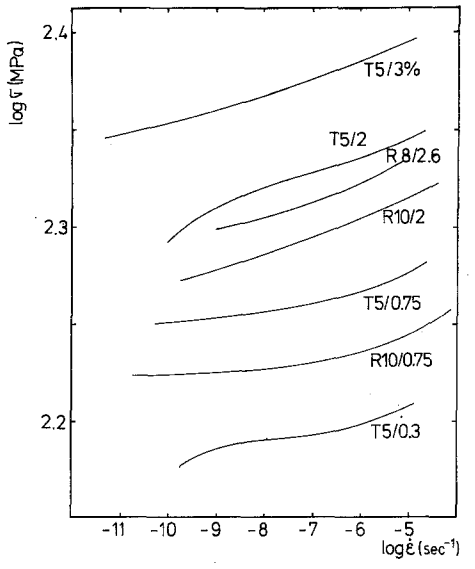

Figure 1 Load relaxation stress–strain rate trajectories for mill-annealed AISI 304 near 563 K, taken from Fig. 6 of [1].

the plastic strain rate in terms of thermally activated dislocation motion is [5]

$$\dot{\epsilon} = \dot{\epsilon}_1 \exp[-\Delta G(\bar{\sigma})/kT] \quad (1)$$

where $\dot{\epsilon}$ is the plastic strain rate, $\dot{\epsilon}_1$ is a general pre-exponential factor, T is the absolute temperature, k is the Boltzmann's constant, ΔG the change in the free enthalpy and $\bar{\sigma}$ is the effective stress. Furthermore, $\bar{\sigma} = \sigma - \sigma_i$ where σ is the applied stress and σ_i an internal stress. If ΔG is expressed as

$$\Delta G(\bar{\sigma}) = \Delta G_0 - \Delta G^m(\bar{\sigma}) \quad (2)$$

Equation 1 can be written as

$$\dot{\epsilon} = \dot{\epsilon}_0 \exp[\Delta G^m(\bar{\sigma})/kT] \quad (3)$$

where

$$\dot{\epsilon}_0 = \dot{\epsilon}_1 \exp(-\Delta G_0/kT)$$

and $\Delta G^m(\bar{\sigma})$ gives the contribution to the change in the free enthalpy due to the applied stress.

As shown by Povolo and Tinivella, [2], the Johnston–Gilman equation,

$$\dot{\epsilon} = \phi\rho \boldsymbol{b} v_0 (\bar{\sigma}/\sigma_0)^{m^*} = \dot{\epsilon}_{J-G}(\bar{\sigma}/\sigma_0)^{m^*} \quad (4)$$

with

$$\dot{\epsilon}_{J-G} = \phi\rho \boldsymbol{b} v_0 \quad (5)$$

where ϕ is an orientation factor, ρ is the mobile dislocation density, $\boldsymbol{b}$ is the Burgers vector and v_0, σ_0 and m^* are material constants, can be written in the form of Equation 3 if

$$\Delta G^m(\bar{\sigma})|_{J-G} = m^* kT \ln(\bar{\sigma}/\sigma_0) \quad (6)$$

and

$$\dot{\epsilon}_0 = \phi\rho \boldsymbol{b} v_0 = \dot{\epsilon}_{J-G} \quad (7)$$

Furthermore, as also shown by Povolo and Tinivella [2], Hart's equation for high homologous temperatures,

$$\dot{\epsilon} = \dot{\epsilon}_H [\ln(\sigma^*/\sigma)]^{-1/\lambda} \quad (8)$$

where σ^* is a hardness parameter, λ is a temperature-independent parameter and $\dot{\epsilon}_H$ depends on temperature, heat treatment and deformation, can be written in the form of Equation 3 if

$$\Delta G^m(\bar{\sigma})|_H = -\frac{kT}{\lambda} \ln[\ln(\sigma^*/\sigma)] \quad (9)$$

and

$$\dot{\epsilon}_0 = \dot{\epsilon}_H \quad (10)$$

The activation volume, defined by

$$V^* = -\partial \Delta G^m(\bar{\sigma})/\partial \bar{\sigma}|_T \quad (11)$$

in the case of Johnston–Gilman equation reduces to

$$V^* = kTm^*/\bar{\sigma} \quad (12)$$

By following the fitting procedure described in [2] it can be shown that the curves with concave upward curvature in Fig. 1 can be well described by the Johnston–Gilman equation (Equation 4), with the parameters given in the first five rows of Table I. The activation volumes, obtained using Equation 12 and the parameters given in Table I, are shown in Fig. 2 as $V^*/\boldsymbol{b}^3$ plotted against $\bar{\sigma}$. The activation volumes obtained during stress–relaxation in bending, at 773 K, for cold-rolled (Σ = 220 MPa) and cold-rolled plus solution annealed 1 h at 1201 K plus aged 16 h at 993 K (Σ = 223 MPa) Type 304 steel are also shown in Fig. 2 for a comparison. Σ indicates the initial stress at the surface of the bent beam before relaxation. The corresponding parameters are given in rows 6 and 7 of Table I.

The stress relaxation data reported by Povolo and Tinivella [2] showed only concave upward or concave downward stress relaxation $\log\sigma$–$\log\dot{\epsilon}$ trajectories and were interpreted either in terms of Equation 4 or Equation 8. As shown in Fig. 1, however, a mixed curvature was observed for specimens T5/0.3% and T5/2%. The interpretation of these two curves will be based on the following argument: it will be assumed that the stress relaxation curves are described actually by Equation 3 with unknown $\Delta G^m(\bar{\sigma})$ and $\dot{\epsilon}_0$. In the region where an upward curvature is present, Equation 3 reduces to Equation 4 and the data are described

TABLE I Parameters obtained by fitting the log σ–log $\dot{\epsilon}$ curves of Fig. 1 either to Equation 4 or to Equation 8. The values obtained during stress relaxation in bending at 773 K are also given for comparison

Curve	σ_i (MPa)	$\dot{\epsilon}_{J-G}\left(\frac{\sigma_i}{\sigma_0}\right)^{m^*}$ (sec^{-1})	m^*	λ	σ^* (MPa)	$\dot{\epsilon}_H$(sec^{-1})	σ_0 (MPa)
T5/0.75%	177.3	3.69	4.77				
T5/3%	206.4	8.1×10^4	14.6				
R10/0.75%	166.6	8.3	4.68				
R10/2%	175.2	4.5×10^4	14.12				
R8/2.6%	189.7	107	8.3				
$\Sigma = 220$ MPa	0	–	4.6				
$\Sigma = 223$ MPa	97.8	7.4×10^{-7}	5.8				
T5/0.3%	153	2.9	4.36	0.60	155.4	6.4×10^{-13}	0.20
T5/2%	206.4	239	6.91	0.22	216.8	2.8×10^{-15}	0.72

by the Johnston–Gilman equation. In the region where the curves show downward curvature, Equation 3 reduces to Equation 8 and the data are described by Hart's equation for high homologous temperatures. These arguments are shown graphically in Fig. 3 where the points have been obtained from the actual experimental curves shown in Fig. 1. The full curves indicate the region where Equation 3 reduces to Equation 4 and the broken curves the region where Equation 3 reduces to Equation 8. There will be a transition region where the experimental curve changes curvature, i.e. where the experimental data can be described both by Equations 4 and 8.

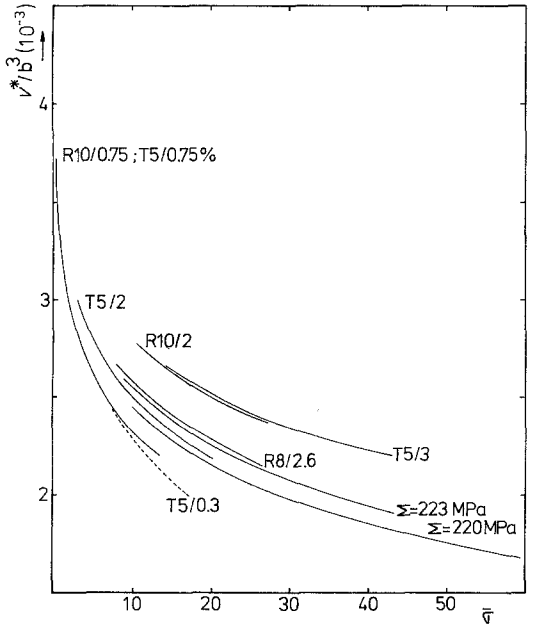

Figure 2 Activation volumes plotted against the effective stress for the relaxation curves of Fig. 1. The results obtained by stress–relaxation in bending, at 773 K, in cold-rolled (Σ = 220 MPa) cold-rolled + solution annealed + aged (Σ = 223 MPa) AISI 304 are shown for a comparison.

As indicated in Fig. 3, there is only a transition point for the curve T5/2%, characterized by the critical stress $\sigma_c = 210.9$ MPa. For curve T5/0.3% the transition region is described by $154.3 \leqslant \sigma_c \leqslant 155.2$ MPa. It is clear that $\sigma_i \leqslant \sigma_c \leqslant \sigma^*$. Furthermore, in the transition region

$$\Delta G^m(\bar{\sigma})|_{J-G} = \Delta G^m(\bar{\sigma})|_H$$
$$\dot{\epsilon}_H = \dot{\epsilon}_{J-G} \quad (13)$$

and the activation volume can also be expressed by [2]

$$V^* = \frac{m^* kT}{\sigma_0} [\ln(\sigma^*/\sigma)]^{1/\lambda m^*} \quad (14)$$

On equating Equations 14 and 12 it is easy to show that at the critical stress

$$\sigma_0 = (\sigma_c - \sigma_i)[\ln(\sigma^*/\sigma_c)]^{1/\lambda m^*} \quad (15)$$

The parameters obtained for curves T5/0.3% and T5/2% by fitting them in the way described in Fig. 3 are given in the last two rows of Table I. The detailed fitting procedure is described elsewhere [2]. σ_0 obtained using Equation 15, the parameters given in Table I and the values of σ_c given in Fig. 3 are also included in Table I. For curve T5/0.3%, since due to the graphical procedure σ_c is not unambigously defined, an average value was used to calculate σ_0 given in Table I. In any case, the value chosen for σ_c will not change the results substantially. A numerical procedure to determine σ_0 will be described elsewhere [6].

Equation 4 reduces to Equation 8 if the internal stress changes according to the law [2]

$$\sigma_i = \sigma - \sigma_0[\ln(\sigma^*/\sigma)]^{-1/\lambda m^*} \quad (16)$$

for $\sigma < \sigma^*$. The internal stresses for all the curves of Fig. 1 are shown in Fig. 4 as a function of the

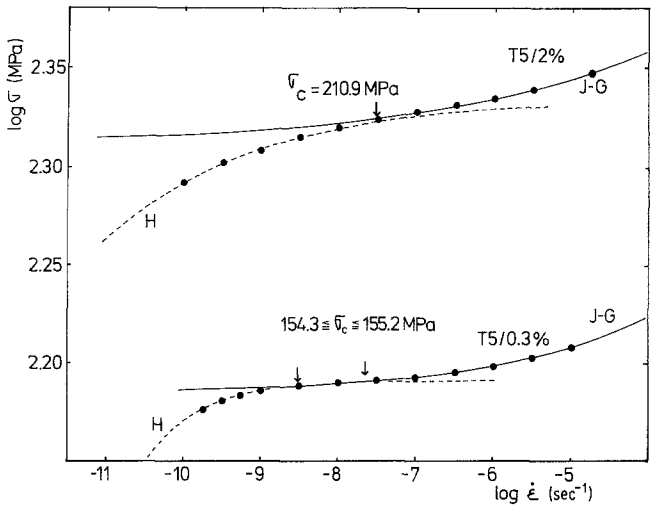

Figure 3 Fitting of the experimental T5/0.3% and T5/2% curves of Fig. 1 (full circles) to the Johnston–Gilman (full curves) and Hart's equation (broken curves). The stresses at which both equations describe the experimental data, σ_c, are indicated.

applied stress. The internal stresses for curves T5/0.3% and T5/2% have been calculated with Equation 16 for $\sigma \leqslant \sigma_c$ and the parameters given in Table I. The corresponding activation volumes, calculated either by using Equation12 or 14 are shown in Fig. 2 as V^*/b^3 plotted against $\bar{\sigma}$.

Finally, plots of $\Delta G^m(\bar{\sigma})/kT$ against $\bar{\sigma}$ for T5/0.3% and T5/2% are shown in Fig. 5. These curves can be obtained by using either Equation 6 or 9 and the parameters given in Table I. The stress dependence of σ_i , shown in Fig. 4, should be taken into account when calculating $\Delta G^m(\sigma)$ with Equation 6. A similar calculation for the rest of the curves of Fig. 1 is not possible since σ_0 cannot be determined.

3. Discussion

From Table I it can be seen that m^* does not remain constant for all the stress relaxation curves, indicating that even the curves described by the Johnston–Gilman equation with constant σ_i cannot be related by scaling [7, 8], i.e. the curves do not translate on to a master stress–strain rate trajectory.

An important point to be stressed is the fact that the data have been interpreted in terms of a general equation (Equation 3) describing thermally activated plastic deformation. When the experimental curves can be described either by the Johnston–Gilman or by Hart's equation, it means only that the general equation reduces to these particular cases. The particular equations are used only to obtain the physical parameters involved in Equation 3. Furthermore, since the physical parameters ΔG^m and V^* must change continuously along a given stress–relaxation curve, in the case

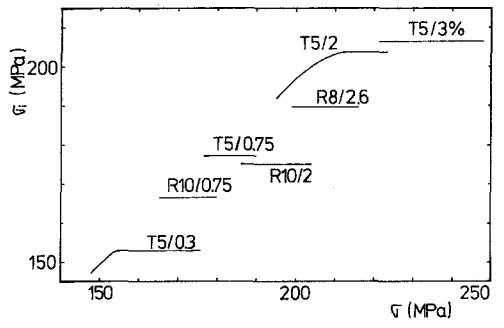

Figure 4 Internal stresses plotted against the applied stress for the log σ–log $\dot{\epsilon}$ curves of Fig. 1.

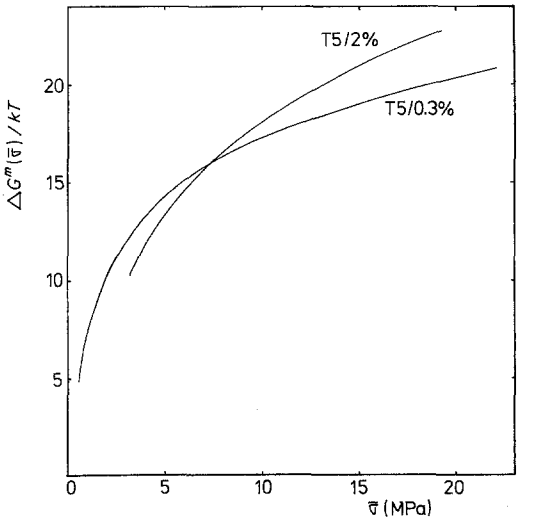

Figure 5 Free activation enthalpy plotted against the effective stress for curves T5/0.3% and T5/2% of Fig. 1.

of curves T5/0.3% and T5/2% it is possible to relate the empirical parameters of Hart's equation with those of the Johnston–Gilman equation. When this correlation is possible, i.e. when the stress relaxation curves present a mixed concavity, ΔG^m and V^* can be determined for the whole curve. This is not the case when the stress relaxation curves with only one type of concavity are measured, as for the data reported by Povolo and Tinivella [2] or for the concave upward curves of Fig. 1. In fact, when the curves are concave upward and can be described by Equation 4, V^* can be determined using Equation 12 but Equation 16 cannot be used to determine ΔG^m since σ_0 is unknown. If the curves are concave downward and can be described by Equation 8, ΔG^m can be determined using Equation 9 but σ_i and V^* remain unknown (see Equations 14 and 15).

Since Hart's equation can be considered as a particular case of the Johnston–Gilman equation with a stress-dependent internal stress, the empirical parameters σ^*, $\dot{\epsilon}_H$ and λ of Equation 8 can be related to the more physical parameters of Equation 4. According to Equations 13 and 5, $\dot{\epsilon}_H = \phi\rho b v_0$ which shows that $\dot{\epsilon}_H$ is related to the dislocation density and, consequently, should be strongly dependent on the thermomechanical treatment as actually observed. Furthermore, from the values reported in Table I it is easy to show that the condition expressed by Equation 13 is satisfied. σ^* can be interpreted as the maximum value that can be reached by the internal stress. The physical significance of λ is difficult to establish since it is related to σ_i, m^*, σ^* and σ_0 in a complicated way. On differentiating Equation 16 and when $\ln \sigma^* \gg \ln \sigma$ it is easy to show that

$$\left.\frac{\partial \ln \bar{\sigma}}{\partial \ln \sigma}\right|_T = 1/\lambda m^* \ln \sigma^* \qquad (17)$$

so that λ is related to the slope of the linear variation of $\ln \bar{\sigma}$ with $\ln \sigma$ at low applied stresses. In addition, on differentiating Equation 9 and imposing the condition $\ln \sigma^* \gg \ln \sigma$ leads to

$$\left.\frac{\partial \ln V^*}{\partial \ln \sigma}\right|_T = -1/\lambda m^* \ln \sigma^* \qquad (18)$$

Comparing Equations 17 and 18 leads to

$$\bar{\sigma} V^* = \text{constant}$$

Then, when the data are described by Hart's equation the product of the activation volume and the effective stress remains constant, at low stresses.

In the simple model used it was assumed that the dislocation density remains constant during each relaxation. Even if this is a strong assumption, reasonable values are obtained for the activation volumes when dislocation motion is controlled mainly by the interactions with precipitates. This is also the case for the values of the activation free enthalpies shown in Fig. 5. It should be pointed out that both V^* and ΔG^m represent average values for the material and not the magnitudes associated with a specific obstacle.

In summary, the stress relaxation curves of Fig. 1 show that in some cases the internal stress does not remain constant during relaxation, due to an evolution of the structure. It is clear that further work is needed to substantiate this conclusion and the model used in this paper.

4. Conclusions

The stress relaxation behaviour of mill-annealed AISI 304 near 563 K can be represented by a general equation describing thermally activated dislocation motion over precipitates. In different regions of the stress–strain rate curves the general equation can be reduced to certain expressions which allow a determination of the physical parameters involved.

Finally, it has been shown that for some stress-relaxation curves the internal stress does not remain constant during relaxation.

Acknowledgement

This work was supported partially by the "Proyecto Multinacional de Technologia de Materiales" OAS-CNEA and the CIC.

References

1. M. J. ANCIAUX, *Met. Trans. A* **12A** (1981) 1981.
2. F. POVOLO and R. TINIVELLA, *J. Mater. Sci.* submitted for publication.
3. W. G. JOHNSTON and J. J. GILMAN, *J. Appl. Phys.* **30** (1959) 139.
4. E. W. HART, *Trans. J. Eng. Mater. Technol.* **98** (1976) 193.
5. U. F. KOCKS, A. S. ARGON and M. F. ASHBY, *Prog. Mater. Sci.* **19** (1975) 303.
6. F. POVOLO and G. H. RUBIOLO, to be published.
7. F. POVOLO and A. J. MARZOCCA, *J. Mater. Sci.* **18** (1983) 1426.
8. *Idem, Trans. Jpn. Inst. Met.* **24** (1983) 111.

Received 26 July
and accepted 21 September 1983